*Desalination and Water Treatment*
www.deswater.com
doi: 10.1080/19443994.2013.809024

52 (2014) 3432–3444
April

Taylor & Francis
Taylor & Francis Group

# Photocatalytic effect of β-cyclodextrin on semiconductors for the removal of Acid Violet dye under UV light irradiation

Subramanian Rajalakshmi, Sakthivel Pitchaimuthu, Nagarathinam Kannan, Ponnusamy Velusamy*

*Centre for Research and Post-Graduate Studies in Chemistry, Ayya Nadar Janaki Ammal College, Sivakasi 626 124, Tamilnadu, India*
*Tel. +91 9443572149; Fax: +91 04562 254970; email: velusamyanjac@rediffmail.com*

Received 9 January 2013; Accepted 21 April 2013

ABSTRACT

This study describes an experimental method for the evaluation of the photodecoloration efficiency of Acid Violet (AV) dye under UV light irradiation by comparing $TiO_2$, ZnO, $TiO_2$/β-cyclodextrin ($TiO_2$/β-CD), and ZnO/β-CD. The effects of concentration of dye, pH, and dose of the catalyst on photodecoloration efficiency were assessed. The mechanism for photodecoloration of AV dye under UV light irradiation was proposed. From the results, it is established that photodecoloration efficiency was doubled with $TiO_2$/β-CD and ZnO/β-CD than compared with pure $TiO_2$ and ZnO. Photocatalytic decoloration efficiency is increased from 80 to 95% with $TiO_2$/β-CD and ZnO/β-CD. Kinetics results showed that the photocatalytic decoloration of AV dye follows pseudo-first-order kinetics. Photo decoloration efficiency of ZnO/β-CD was higher than $TiO_2$/β-CD. The catalysts were characterized by X-ray diffraction (XRD), field emission-scanning electron microscopy (FE-SEM), and ultraviolet-diffuse reflectance spectroscopy (UV-DRS) analyses. FE-SEM analysis showed that there is no change in surface morphology in $TiO_2$/β-CD and ZnO/β-CD systems compared to bare $TiO_2$ and ZnO systems. XRD analysis shows that the crystalline features does not change by addition of β-CD. UV-DRS analysis showed that band gap energy of ZnO/β-CD system is higher than other catalytic systems. Therefore, ZnO/β-CD adsorbs more light photons than other systems. Optical thickness measurements showed that 2 g/L of catalysts is optimum for the photocatalytic decoloration process. Fourier transform infrared spectroscopy (FT-IR), UV–visible analysis and $^1$H NMR analyses confirm the formation of inclusion complex between AV dye and β-CD. The $^1$H NMR analysis of β-CD showed that the phenyl ring of AV dye is protruded into β-CD cavity.

*Keywords:* Acid Violet dye; COD; Photo decoloration efficiency; $TiO_2$/β-CD and ZnO/β-CD

## 1. Introduction

The treatment of industrial wastewaters for removing organic pollutants is one of the very important aspects of environmental technology. Consequently, a growing interest in heterogeneous photocatalysis, as an advanced oxidation technique (AOT), has been developed. The use of nanocrystalline semiconductors as photocatalysts, to initiate interfacial redox reactions,

*Corresponding author.

has generated greater interests, due to their unique physicochemical properties, caused by their nanosized dimensions and higher surface/volume ratio. In this context, Titanium dioxide ($TiO_2$) has been investigated as the most promising photocatalyst for the treatment of organic as well as inorganic pollutants, from water and air, since it has a reasonable photoactivity under ultraviolet light irradiation (anatase, Eg = 3.2 eV). $TiO_2$ is not toxic, water insoluble, and comparatively inexpensive [1–5].

In recent years, nanostructured ZnO has attracted a great deal of attention, owing to its unique and novel applications in the optics, optoelectronics, catalysis, pyroelectricity, and piezoelectricity. ZnO is known to be one kind of the important photocatalysts because of its unique advantages, such as its low price, high photocatalytic activity, and nontoxicity [6]. In the advanced oxidation of pulp mill bleaching waste water, Zinc Oxide (ZnO) was found to be more efficient catalyst than $TiO_2$ [7]. Another advantage of ZnO is that it absorbs larger fraction of the solar energy than $TiO_2$ [8]. For these reasons, ZnO is considered as the most suitable photocatalyst for photocatalytic oxidation of organic compounds in the presence of light. However, the major limitations for its wide practical application are the small percentage of photons of the solar radiation, which has the required energy to photogenerated electrons and holes, and their high charge recombination rate. On the other hand, the disadvantage of this catalyst is that its catalytic activity is still not high enough for the commercial applications.

Therefore, the development of visible-light-driven photocatalysts with high energy transfer efficiency has become one of the most challenging tasks in these days. Therefore, a number of efforts have been attracted to inhibit the recombination of electron-hole pairs and improve charge transport *via* coupling the wide band gap semiconductor photocatalysts with other materials, such as semiconductor-noble metal composite, quantum dot-semiconductor composite, C–N doped semiconductor, carbon nanotubes (CNTs), or fullerene ($C_{60}$)-semiconductors composites [9–14].

β-Cyclodextrin (β-CD) is a sophisticated material for enhancing the photocatalytic activity of $TiO_2$. Cyclodextrins (CDs) are cyclic oligosaccharides made up of six to eight α-d-glucose units connected through glycosidic α-1, 4 bonds. CDs with six to eight α-d-glucose units are denoted α-, β-, and γ-CDs, respectively. They have the ability to form an inclusion complex with various guest molecules of suitable polarity and dimension because of their unique molecular structure (they possess a hydrophobic internal cavity and hydrophilic external surface). β-CD can be modified as electron-donating and molecular-recognizing agents on semiconductor nanoparticles [15–21]. In order to improve photocatalytic activity of metal oxides (MO) ($TiO_2$ and ZnO), several methods have been developed [22–29]. The modification of β-CD on the semiconductor photocatalyst shows a significant enhancement effect on degradation processes of pollutants [30,31]. Earlier, we have reported the photocatalytic degradation of dyes by $TiO_2$/β-CD and ZnO/β-CD using UV A light irradiation [32,33].

The present works focus on comparison of photodecoloration efficiency of Acid Violet (AV) dye with $TiO_2$, ZnO, $TiO_2$/β-CD, and ZnO/β-CD under UV light irradiation and propose decoloration mechanism for photodecoloration process.

## 2. Experimental procedure

### 2.1. Materials used

AV dye obtained from Loba Chemie [India] was used as such. The catalysts *viz.*, ZnO and $TiO_2$ were received from S.D. Fine Chemicals, India. β-CD was purchased from Hi Media Chemicals (P) Ltd. Structures and physical properties of AV dye and β-CD are presented in Fig. 1 and Table 1. All the other chemicals and reagents were used as received. Photodecoloration experiments were carried out under UV light irradiation (365 nm).

### 2.2. Samples preparation

Reported procedures were employed for the preparation of AV-β-CD complex [34]. To a saturated solution of β-CD in distilled water, equimolar amount of AV dye was added and stirred continuously for 24 h. The precipitated inclusion complex was filtered and washed with diethyl ether to remove uncomplexed AV dye and dried in an air oven at 60°C for 2–3 h. The precipitate obtained is used for the characterization of AV–β-CD complex by fourier transform infrared spectroscopy (FT-IR) and $^1$H NMR analyses.

MO such as $TiO_2$ and ZnO were added into 0.01 mol/L β-CD solution and stirred for 20 min. The suspended solution was centrifuged; the solids separated and washed three times with water. The solid was dried with an infrared lamp used for X-ray diffraction (XRD) and field emission-scanning electron microscopy (FE-SEM) analyses [18].

Exactly $1.41 \times 10^{-4}$ M of AV dye was prepared by using deionised water and various concentrations of β-CD like 2.82, 4.23, 5.64, 7.05, and $8.46 \times 10^{-4}$ M were prepared in a 25 mL SMF. These two solutions were mixed thoroughly with magnetic stirrer for 24 h. Then,

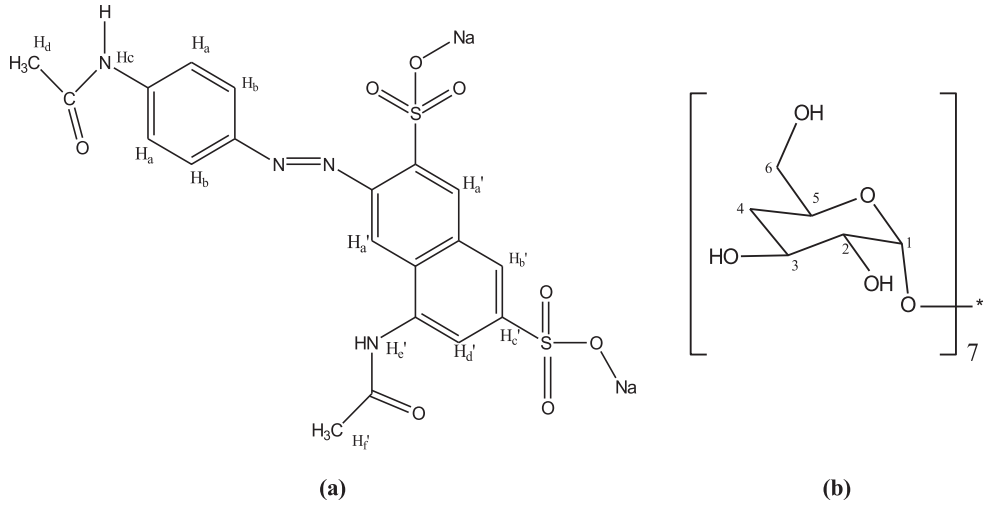


Fig. 1. Structures of (a) AV dye and (b) β-CD.

Table 1
Physical properties of AV dye and β-CD.

| Name | Acid Violet dye | β-CD |
|---|---|---|
| Molecular formula | $C_{20}H_{24}N_4Na_2O_9S_2$ | $C_{42}H_{70}O_{35}$ |
| Molecular weight | 566.47 | 1135.0 |
| Appearance | Violet powder | White powder |
| pH | 3.2 | – |
| $\lambda_{max}$ | 518 nm | – |

these samples were analyzed with UV spectrophotometer [35].

### 2.3. Instruments employed

X-ray diffraction patterns of powder samples were recorded with a high-resolution powder X-ray diffractometer model RICH SIERT & Co with Cu Kα radiation as the X-ray source ($\lambda = 1.5406 \times 10^{-10}$ m). FE-SEM analysis was done using ZEISS scanning electron microscope. UV–vis diffuse reflectance spectra were recorded on a Shimadzu 2550 UV–vis spectrophotometer with $BaSO_4$ as the background between 200 and 700 nm. $^1$H NMR spectra were recorded by a 400 MHz Bruker NMR spectrometer (in DMSO–$d_6$). UV–visible spectrophotometer (Shimadzu UV-1700) and the scan range were from 400 to 700 nm. FT-IR spectra were recorded using FT-IR spectrometer (Shimadzu model 8400S) in the region 4,000–400 $cm^{-1}$ using KBr pellets. Absorbance of the dye was determined with visible spectrophotometer (ELICO-207). The pH of the dye solution was measured by using digital pen pH meter (HANNA instrument, Portugal).

### 2.4. Methods adopted

Heber multilamp photo reactor (HML MB 88) with eight lamps was employed as UV radiation source. The lamp emits UV radiation mainly at 365 nm with a power output of 30 W. The distance between the UV source and the sample holder is 5 cm. The glass tubes with 60 ml capacity were used as sample holder. The pH values of AV dye solutions were adjusted using digital pen pH meter depending on desired values with 0.1 N HCl and 0.1 N NaOH solutions as their effect on the properties of adsorption surface of MO is negligible. Prior to irradiation, MO suspensions were kept in dark for 10 min. to attain adsorption–desorption equilibrium between dye and MO systems. During irradiation, the reactant solutions were continuously stirred with magnetic stirrer. The tubes were taken out at different intervals of time and the solution was centrifuged well. The supernatant liquid was collected and labeled for the determination of concentrations for the remaining dye by measuring its absorbance (at $\lambda_{max} = 518.0$ nm) with Visible spectrophotometer. In all the cases, exactly 50 mL of reactant solutions were irradiated with required amount of

respective catalyst either $TiO_2$ or ZnO. The pH of the AV dye solutions were adjusted before irradiation process and it was not controlled during the course of the reaction. The experiment was carried with solution pH (3.2) and the irradiation time was fixed as 120 min.

By keeping the concentrations of AV dye-β-CD as constant with the molar ratio of 1:1, the effect of all other experimental parameters on the percentage of photocatalytic decoloration of AV dye solution was investigated.

### 2.5. Determination of chemical oxygen demand (COD)

Exactly 50 mL of the sample was taken in a 500 mL round bottom flask with 1 g of mercuric sulfate. Slowly, 5 mL of silver sulfate reagent (prepared from 5.5 g silver sulfate per kg in concentrated sulfuric acid) were added to the solution. Cooling of the mixture is necessary to avoid possible loss of volatile matters if any, while stirring. Exactly 25 mL of 0.25 N potassium dichromate solution was added to the mixture slowly. The flask was attached to the condenser and 70 mL silver sulfate reagent was added and allowed to reflux for 2 h. After refluxtion, the solution was cooled at room temperature. Five drops of Ferroin indicator were added and titrated against a standard solution of Ferrous Ammonium Sulfate (FAS) until the appearance of the first sharp color change from bluish green to reddish brown. The COD values can be calculated in terms of oxygen per liter in milligram (mg $O_2$/l) using the following equation [36].

$$\text{COD mg } O_2/1 = (B - A) \times N \times 8,000/S \quad (1)$$

where, $B$ is the volume of FAS consumed by $K_2Cr_2O_7$ (ml), $A$ is the volume of FAS consumed by $K_2Cr_2O_7$ and AV dye mixture (ml), $N$ is the normality of FAS, and $S$ the volume of the AV dye.

## 3. Results and discussion

### 3.1. X-ray powder diffraction analysis

The X-ray powder diffraction patterns of β-CD, $TiO_2$, $TiO_2$/β-CD, ZnO, and ZnO/β-CD are presented in Fig. 2(a)–(e), respectively. The XRD patterns of $TiO_2$/β-CD and ZnO/β-CD systems are similar to that of $TiO_2$ and ZnO particles. This indicates that the incorporation of β-CD on MO does not change the crystalline structure of the neat $TiO_2$ and ZnO. But, the main peak intensity of the both $TiO_2$/β-CD and ZnO/β-CD system is slightly lower than bare $TiO_2$ and ZnO. The results are in accordance with JCPDS files # 21-1272 ($TiO_2$) [33] and # 36-1451 (ZnO) [37].

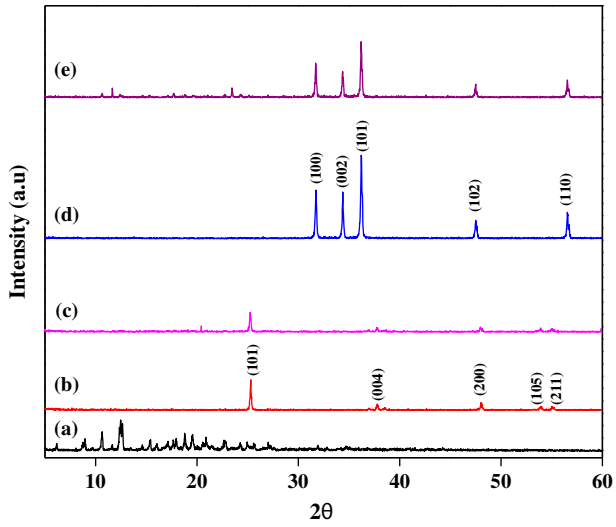


Fig. 2. XRD Pattern for (a) β-CD (b) $TiO_2$ (c) $TiO_2$/β-CD (d) ZnO and (e) ZnO/β-CD.

### 3.2. FE-SEM analysis

Fig. 3(a)–(e) depicts FE-SEM of β-CD, $TiO_2$, ZnO, $TiO_2$/β-CD, and ZnO/β-CD, respectively. The surface morphology of pristine β-CD (Fig. 3(a)) shows its amorphous nature. $TiO_2$ (Fig. 3(b)) has spherical morphology with uniform particle size. ZnO (Fig. 3(c)) has prismatic morphology with uniform particles containing wurtzite lattice structure, whereas in $TiO_2$/β-CD (Fig. 3(d)) and ZnO/β-CD (Fig. 3(e)) systems, two different types of particles are observed. The smaller size particles correspond to β-CD and larger particles correspond to MO such as $TiO_2$ and ZnO. This indicates that the β-CD molecules are adsorbed on the surface of the MO. It is also observed that the surface of metal oxide systems ($TiO_2$/β-CD and ZnO/β-CD) are very loosely packed in nature. This kind of surface can provide a better adsorption environment and more active sites for the photocatalytic decoloration reactions.

### 3.3. UV-DRS studies

The ultraviolet-diffuse reflectance spectroscopy (UV-DRS) spectra of $TiO_2$, ZnO, $TiO_2$/β-CD, and ZnO/β-CD are shown in Fig. 4(a)–(d). It shows that the absorption is maximum at wavelength near 350–400 nm. It was found that the band gap energy of ZnO/β-CD system is found to be higher than other catalytic systems such as $TiO_2$, ZnO, and $TiO_2$/β-CD. Furthermore, $TiO_2$/β-CD and ZnO/β-CD systems have slight higher absorption intensities than bare $TiO_2$ and ZnO, respectively. Thus, photocatalytic activities of ZnO/β-CD as well as $TiO_2$/β-CD systems are higher than their bare catalysts.

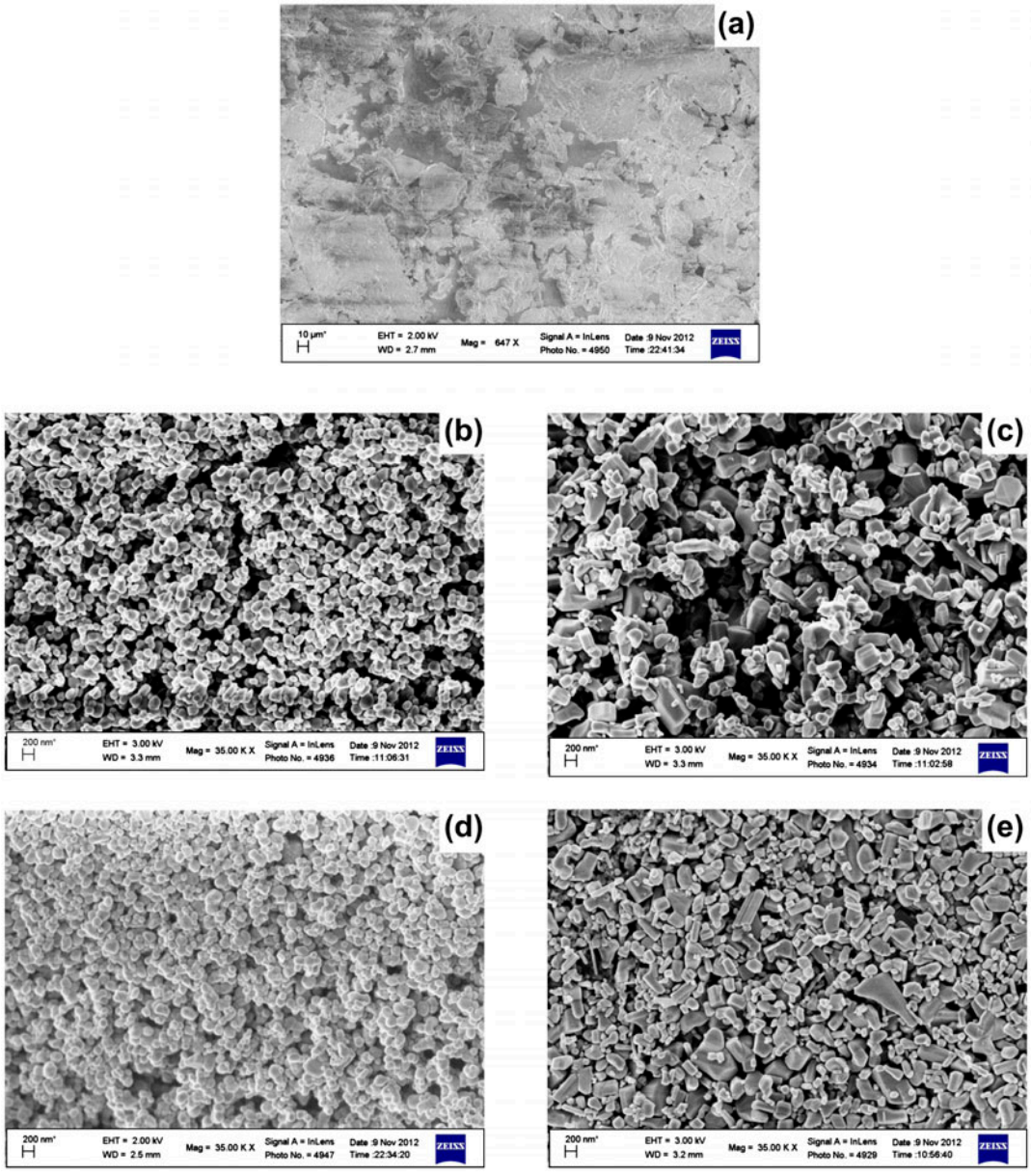


Fig. 3. FE-SEM analysis of (a) β-CD (b) $TiO_2$ (c) ZnO (d) $TiO_2$/β-CD and (e) ZnO/β-CD.

### 3.4. Dissociation constant measurement

The UV–visible spectra of complexation of AV dye with β-CD are clearly illustrated in Fig. 5a. The increase in the absorbance of dye molecule with the increase of concentration of β-CD reveals that, there is a strong inclusion between β-CD and dye molecules which leads to the fact the β-CD accommodates enough dye molecules inside its cavity [38]. The dissociation constant ($K_D$) value for the complexation between β-CD and dye can be calculated using the Benesi–Hildebrand equation [39].

$$[C][S]/\Delta OD = [C] + [S]/\Delta\varepsilon + K_D/\Delta\varepsilon \quad (2)$$

where [*C*] and [*S*] represent the concentrations of the host and guest molecules, respectively, at equilibrium. ΔOD = increase in absorption upon addition of β-CD; $\Delta\varepsilon$ = difference in molar extinction coefficients between the bound and the free guest (dye) molecule. $K_D$ = dissociation constant.

$K_D$ can be obtained from the ratio of the intercept ($K_D/\Delta\varepsilon$) and the slope ($1/\Delta\varepsilon$) from the linear plot of [*C*] [*S*]/ΔOD *vs* {[C] + [S]} (Fig. 5b). The determined $K_D$ value is $1.46 \times 10^{-4}$ M.

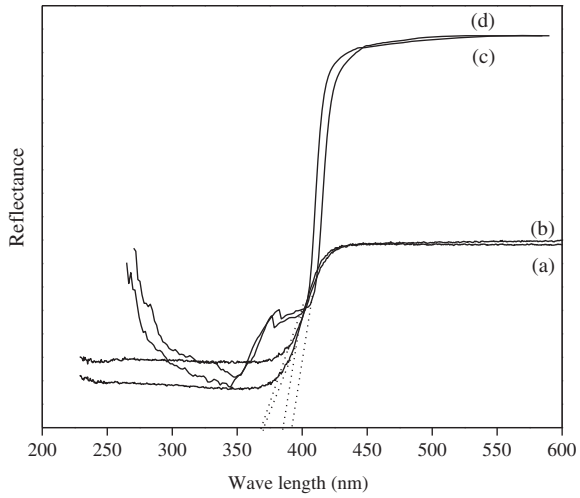


Fig. 4. UV-DRS Spectra of (a) $TiO_2$ (b) $TiO_2$/β-CD (c) ZnO and (d) ZnO/β-CD.

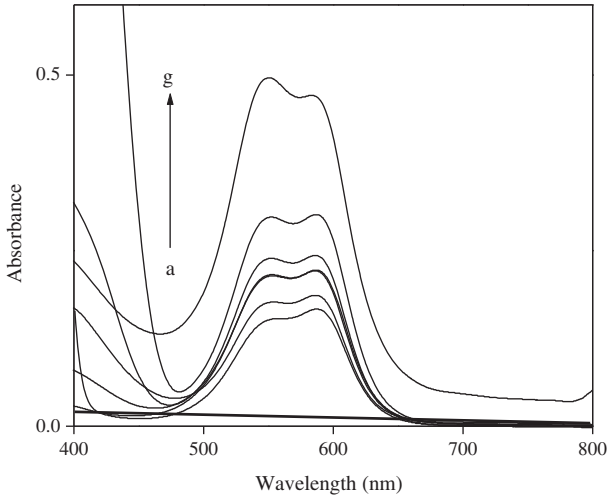


Fig. 5a. UV–visible spectra for complexation AV 7/β-CD. (a) β-CD (b) AV 7 (c) 1:1 AV 7/β-CD (d) 1:2 AV 7/β-CD (e) 1:3 AV 7/β-CD (f) 1:4 AV 7/β-CD (g) 1:5 AV 7/β-CD.

### 3.5. FT-IR spectral analysis

FT-IR spectra of complexation between AV dye, β-CD, 1:1 physical mixture of β-CD, and AV dye and 1:1 complex mixture of β-CD and AV dye are presented in Fig. 6(a)–(d). Comparing the FT-IR spectra of AV dye, β-CD, AV dye/β-CD physical mixture, and AV dye/β-CD 1:1 complex, it is clearly understood that there will be shifts in the peaks corresponding to –NH stretching (3382.91 $cm^{-1}$), $C_6H_5$–CO–NH–$CH_3$ stretching (3205.47 $cm^{-1}$), combination of –C=O and –NH stretching (2933.53 $cm^{-1}$), –N=N stretching (2044.3 $cm^{-1}$) and $SO_3^-$ stretching (1029.92 $cm^{-1}$) in complex mixture. This confirms the formation of a strong inclusion complex between β-CD and AV dye molecules, which enhance the decoloration of dye molecules by suitable semiconductors.

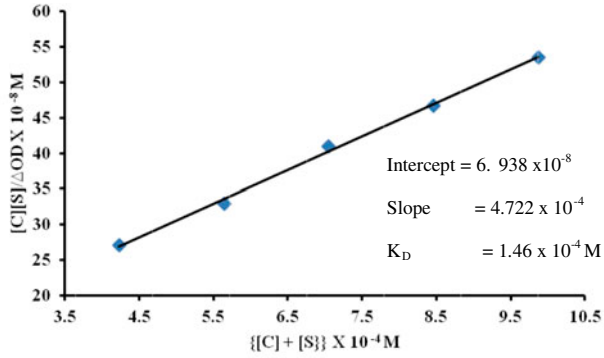


Fig. 5b. Determination of $K_D$.

### 3.6. $^1H$ NMR analysis

Direct evidence for the formation of inclusion complex can be obtained from $^1H$ NMR spectra. Fig. 7 showed the typical $^1H$ NMR spectra of inclusion complex of AV with β-CD in DMSO-$d_6$. The significant shifts in $^1H$ NMR spectra strongly confirmed the formation of inclusion complex. The values of chemical shifts, $\delta$ for different protons in β-CD and AV–β-CD inclusion complex, are listed in Table 2. It can be seen from the $^1H$ NMR that in inclusion complex, an upfield shift was occurred for $H_3$ and $H_5$, which locate in the inner side of β-CD. The shift of chemical shift

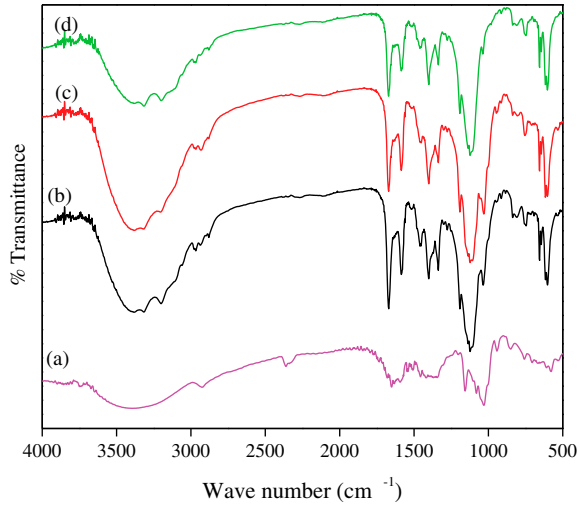


Fig. 6. FT-IR spectral analysis of (a) β-CD (b) AV (c) physical mixture of β-CD with AV and (d) complexation mixture of AV with β-CD.

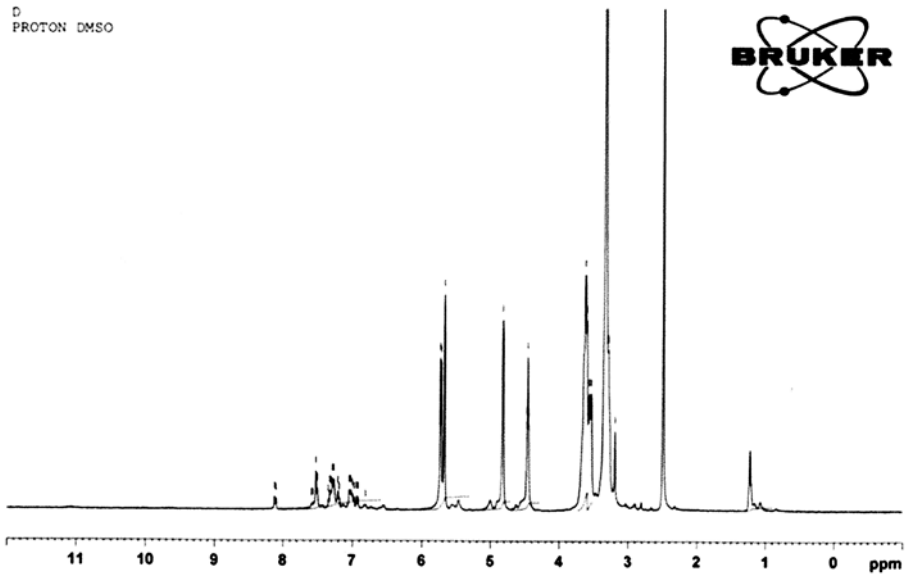


Fig. 7. $^{1}H$ NMR spectra of AV-β-CD inclusion complex.

Table 2
Chemical shift $\delta$ and $\Delta\delta$ of protons of β-CD in free host and inclusion complex

| | $H_1$ | $H_2$ | $H_3$ | $H_4$ | $H_5$ | $H_6$ |
|---|---|---|---|---|---|---|
| β-CD | 5.03 | 4.00 | 3.73 | 3.02 | 3.73 | 3.54 |
| AV–β-CD | 5.72 | 4.46 | 3.60 | 3.28 | 3.60 | 3.54 |
| $\Delta\delta$ | −0.69 | −0.46 | 0.13 | −0.26 | 0.13 | 0.00 |

Chemical shifts values are expressed in ppm.

Table 3
Chemical shift $\delta$ and $\Delta\delta$ of protons of AV in free guest and inclusion complex

| | $H_a$ | $H_b$ | $H_c$ | $H_d$ |
|---|---|---|---|---|
| AV | 7.84 | 7.91 | 8.0 | 2.02 |
| AV–β-CD | 7.52 | 7.59 | 8.1 | 2.30 |
| $\Delta\delta$ | 0.32 | 0.32 | −0.1 | −0.28 |

Chemical shifts values are expressed in ppm.

($\Delta\delta$) of $H_3$ and $H_5$ suggested that the AV dye molecules encapsulated into the hydrophobic cavity of β-CD. On the contrary, the chemical shifts of $H_1$, $H_2$, and $H_4$ which are on the outer surface of β-CD and the narrow opening of β-CD undergo downfield shift due to the interaction between β-CD and the AV dye molecules. $H_6$ proton does not undergo any changes. Similarly, the chemical shifts of $H_a$ and $H_b$ of AV dye are also shifted to upfield and $H_c$ and $H_d$ shifted to downfield significantly because of the interaction between AV and β-CD (Table 3). The above chemical shift behavior for the β-CD protons establishes that the phenyl ring of AV dye is positioned within the β-CD cavity [40,41].

### 3.7. Optical thickness

The optical thickness of the sample holder was evaluated for the catalysts such as $TiO_2$, ZnO, $TiO_2$/β-CD, and ZnO/β-CD systems with change in amount of catalysts and given in Table 4. It has been observed that optical thickness of ZnO/β-CD system was less compared to other systems and reduced with increase in dose of the catalysts. The results showed that the 2 g/L is optimum for the photocatalytic decoloration process [42,43].

Table 4
Optical thickness of the sample holder

| Catalysts | Optical thickness | | | | |
|---|---|---|---|---|---|
| | 1 g/L | 2 g/L | 3 g/L | 4 g/L | 5 g/L |
| $TiO_2$ | 3.4 | 2.8 | 2.5 | 1.9 | 1.5 |
| ZnO | 3.0 | 2.6 | 2.0 | 1.6 | 1.2 |
| $TiO_2$/β-CD | 2.8 | 1.8 | 1.5 | 1.2 | 1.1 |
| ZnO/β-CD | 2.4 | 1.0 | 1.0 | 1.0 | 1.0 |

### 3.8. Effect of initial dye concentration

The effect of initial AV dye concentration on the photocatalytic decoloration process was investigated by treating different initial concentrations of AV dye:

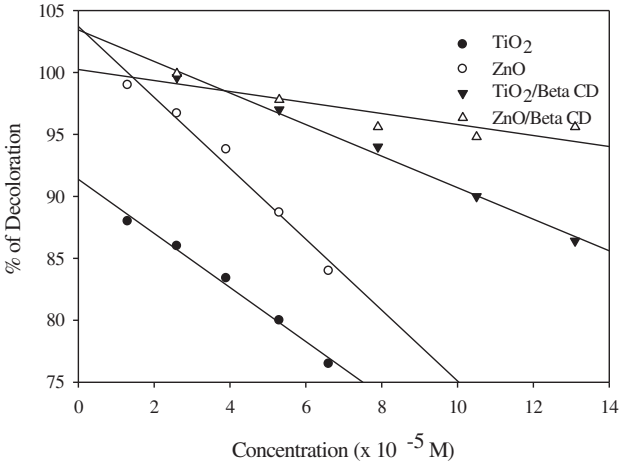


Fig. 8. Effect of initial concentration on photocatalytic decoloration of AV dye under UV light irradiation. Time = 120 min; Dose = 2 g/L; pH = 3.2.

1.3, 2.6, 3.9, 5.3, and $6.6 \times 10^{-5}$ M for $TiO_2$ and ZnO and 2.6, 5.3, 7.9, 10.5, and $13.1 \times 10^{-5}$ M for $TiO_2$/β-CD and ZnO/β-CD at pH 3.2 and with catalyst amount of 2 g/L. Fig. 8 shows a qualitative description of percentage of decoloration *vs* dye concentration. The percentage decoloration of dye decreased with increasing its initial concentration. The presumed reasons behind the decrease of percentage decoloration of dye molecules can be explained. The increasing coverage of the active sites of catalyst surface with the adsorbed dye molecules may shield the interaction of the composite with the precursor molecules. The UV-screening effect of the dye itself is another factor. At high concentration of the dye, the UV-light may be significantly absorbed by the dye molecules rather than the penetration of photons into the composite surface. This results in less generation of $OH^-$ radical ($E_o = 2.81$ eV) which is a powerful species for the dye decoloration. Similar observations have been reported by other researchers [44,45].

### 3.9. Photocatalytic decoloration kinetics of AV

When photocatalytic decoloration of AV dye was performed in varying initial concentrations, the results demonstrated that conversions were less in the solutions of higher initial AV dye concentrations when compared to the conversions in the lower concentration solutions. This can be ascribed to the decrease in the number of active sites on the catalyst surface due to the covering of the surface with AV molecules which is directly proportional with the initial concentration of AV. The relationship between the initial degradation rate ($r$) and the initial concentration of the organic substrate for heterogeneous photocatalytic decoloration has been described by Langmuir–Hinshelwood. The Langmuir–Hinshelwood model can be written as follows

$$r = k\frac{K_{AV}[AV]}{1 + K_{AV}[AV]_0} = k_{obs}[AV] \quad (3)$$

$$\frac{1}{k_{obs}} = \frac{1}{kK_{AV}} + \frac{[AV]_0}{k} \quad (4)$$

where $[AV]_0$ is the initial concentration of AV dye (M); $K_{AV}$ is the Langmuir–Hinshelwood adsorption equilibrium constant ($M^{-1}$); and $k$ is the rate constant of surface reaction (M $min^{-1}$):

$$\ln C_0/C_t = k_{obs}t \quad (5)$$

$k_{obs}$ values for each initial concentration were found from the slopes of straight line obtained by plotting.

ln ($C_0/C_t$) vs. reaction time (t) (figure not shown.) When initial concentrations were plotted *vs* $1/k_{obs}$, the rate constant and the adsorption equilibrium constant were calculated to be 0.014 mM $min^{-1}$ ($TiO_2$), 0.042 mM $min^{-1}$ (ZnO), 0.082 mM $min^{-1}$ ($TiO_2$/β-CD), and 0.136 mM $min^{-1}$ (ZnO/β-CD) and 44.14, 21.53, 15.58, and 13.36 mM, respectively (Fig. 9) [46].

### 3.10. Effect of amount of catalyst

From an economical point of view, in any decoloration process the amount of catalyst is considered as one of the most important parameters that should be

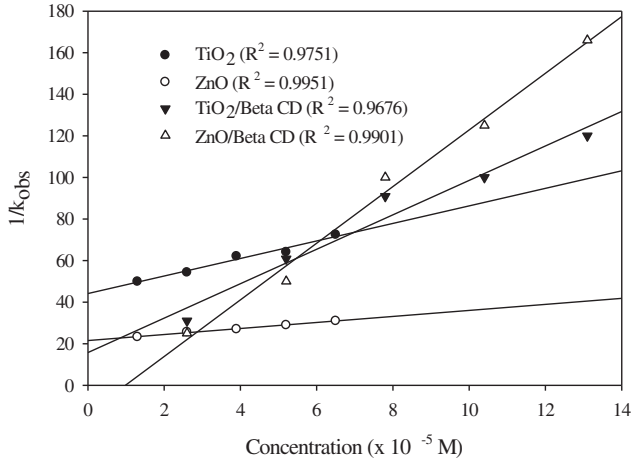


Fig. 9. Determination of the adsorption equilibrium constant and the reaction rate constant for AV dye decoloration.

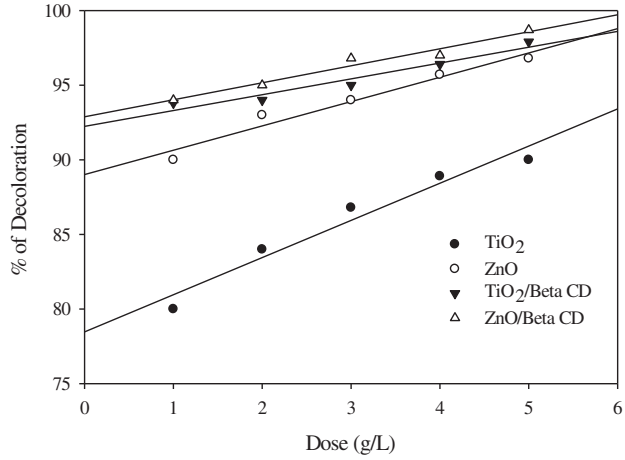


Fig. 10. Effect of dose of the catalysts on photocatalytic decoloration of AV dye under UV light irradiation. Concentration = $3.9 \times 10^{-5}$ M ($TiO_2$ and ZnO), $7.9 \times 10^{-5}$ M ($TiO_2$/β-CD), $10.5 \times 10^{-5}$ M (ZnO/ β-CD); time = 120 min.; pH = 3.2.

investigated. In order to determine the optimum amount of catalyst on the photodecoloration of AV dye, a series of decoloration experiments were conducted by varying the amount of catalysts in the range from 1 to 5 g/L (Fig. 10). The results clearly demonstrate that the optimum catalyst concentration for AV dye decoloration was 2 g/L and photodecoloration efficiency increases with increase in amount of catalysts. This can be explained in terms of availability of active sites on the catalyst surface and the penetration of UV light into the suspension. The total active surface area increases with increasing catalyst dosage [47,48].

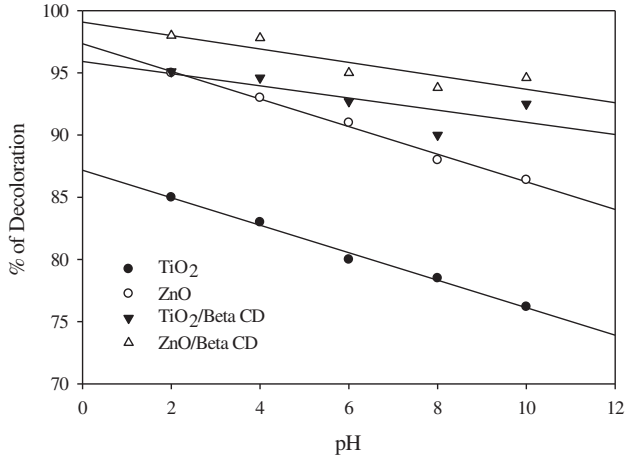


Fig. 11. Effect of pH on photocatalytic decoloration of AV dye under UV light irradiation. Concentration = $3.9 \times 10^{-5}$ M ($TiO_2$ and ZnO), $7.9 \times 10^{-5}$ M ($TiO_2$/β-CD), $10.5 \times 10^{-5}$ M (ZnO/ β-CD); time = 120 min; dose = 2 g/L.

### 3.11. Effect of pH

The pH of the reaction medium seems to represent one of the main parameters that affect the percentage of decoloration, particularly the dye to be degraded may be found at different pHs in colored effluents. The pH dependence of percentage of decoloration was examined at pH ranging from 2 to 10. The dependence of percentage of decoloration upon pH is represented in Fig. 11. The pH has strong inhibitory effect upon the efficiency of dye disappearance. The pH effect is related to the point of zero charge (pzc) of $TiO_2$ at pH 6.2 [49] and ZnO at pH 8.8 [50]. In acidic media the surface of catalyst is positively charged, whereas it is negatively charged under alkaline conditions [51,52] according to the following equations

$$\text{pH<PZC: MO} + \text{H}^{+-} \rightarrow \text{MO}^{2+} \quad (6)$$

$$\text{pH} > \text{PZC: M} - \text{OH} + \text{OH}^{-} \rightarrow \text{MO}^{-} + \text{H}_2\text{O} \quad (7)$$

MO = Metal oxide. Since AV dye is negatively charged due to the sulfonated groups which are ionized in water, their electrostatic attraction to the catalysts surface is favorable in acidic solution, and forbidden in alkaline media due to the columbic repulsion between the negatively charged surface of catalysts and the dye molecules. Thus, the reaction rate reached a maximum value at very low pH. Moreover, the generation of $^{\bullet}OH$ radicals by the effect of UV-light on the catalyst of the composite may also represent a further factor for increasing reaction rate in acidic environment. In acidic medium, photogenerated holes react with water molecule producing hydroxyl radical as given in the following equation

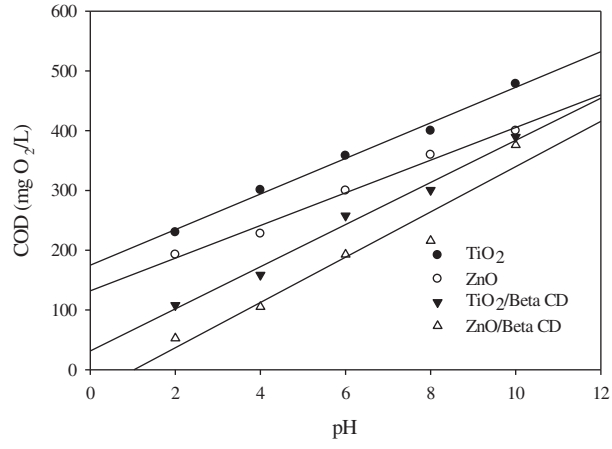


Fig. 12. Determination COD for AV 7 dye under UV light irradiation.

$$H_2O + h^+_{VB} \longrightarrow {}^{\bullet}OH + H^+ \quad (8)$$

Sohrabi and Ghavami [53] reported that in strong alkaline medium (pH > 10), such $^{\bullet}OH$ radicals are rapidly scavenged because in alkaline solution there is a coulombic repulsion between the negatively charged surface of photocatalyst and the hydroxide anions. This fact could prevent the formation of $^{\bullet}OH$ and thus decrease the photo-oxidation and, therefore, the photodecoloration rate decreases [54].

### 3.12. COD removal of treated AV dye solution

Chemical Oxygen Demand (COD) values are related to the total concentration of organics in the solutions. Based on this criterion, the evolution of the initial compound concentration and COD of AV dye solution was determined to evaluate the pollutant elimination after photodecoloration process (Fig. 12). COD results also demonstrated that the reduction in COD values for AV dye increased with increase in pH and results revealed that there could be no formation of harmful products at the end of photocatalytic decoloration reactions.

### 3.13. Comparison of photocatalytic activity of catalysts

In order to understand the efficiency of the catalysts, identical experiments were carried out with $TiO_2$, ZnO, $TiO_2$/β-CD, and ZnO/β-CD on the photocatalytic decoloration of AV dye. The results (Fig. 13) clearly indicate that ZnO/β-CD is found to be the better catalyst for the decoloration of AV dye. The photocatalytic activity of catalyst ZnO/β-CD is higher than $TiO_2$/β-CD, ZnO, and $TiO_2$. It was found from UV-DRS spectra that the band gap energy of ZnO/β-CD (3.35 eV) system was found to be higher than compared to that of other catalytic systems such as $TiO_2$ (3.16 eV), ZnO (3.3 eV) and $TiO_2$/β-CD (3.25 eV). The greater activity of ZnO/β-CD is due to the adsorption of more light quanta than other catalysts. So, the quantum efficiency of ZnO/β-CD is significantly larger and absorbs large fraction of the solar spectrum than other catalysts [55].

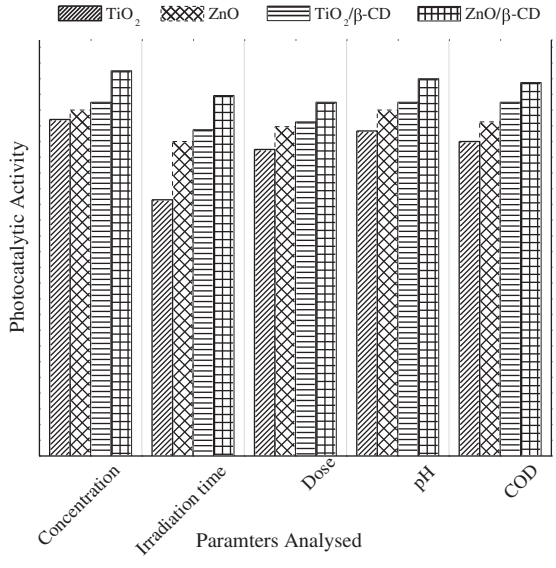


Fig. 13. Comparison of photocatalytic activity of $TiO_2$/β-CD and ZnO/β-CD with $TiO_2$ and ZnO.

### 3.14. Adsorption performance

The adsorptive and photocatalytic performances of $TiO_2$, ZnO, $TiO_2$/β-CD, and ZnO/β-CD were evaluated in AV dye aqueous solution at room temperature. Before UV irradiation, an adsorption processes of AV dye on the samples occur the process proceeds very fast, takes about 5 min close to saturation and 10 min to reach adsorption–desorption equilibration for AV dye samples (Fig. 14). The saturated adsorption amounts on all the catalytic systems are very low, clearly suggesting a weak interaction of MO with AV dye [56].

### 3.15. Mechanism for the enhancement of photocatalytic activity

The mechanism for the photocatalytic decoloration of AV dye with MO/β-CD is schematically represented in Eqs. (i)–(ix). AV dye molecules enter into the cavity of β-CD, which is linked to the MO surface in the equilibrium stage. Since CDs have higher

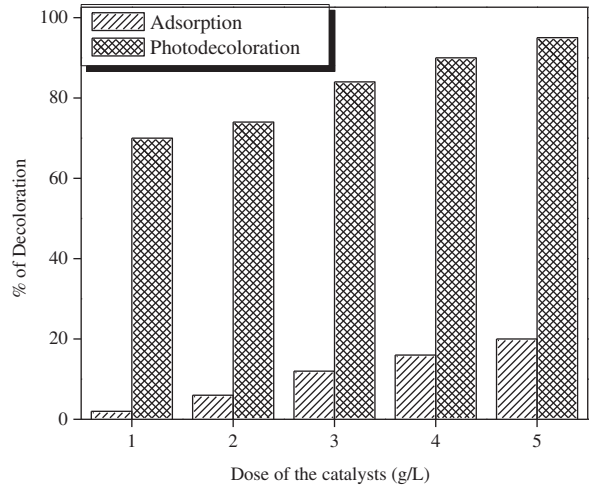


Fig. 14. % of Decoloration *vs* Dose of the catalysts.

affinity on MO surface than AV dye, β-CD molecules could be adsorbed on MO surface and occupy the reaction sites. β-CD would capture holes on active MO surface resulting in the formation of stable MO/β-CD complex. Thus, reaction (ii), the inclusion complex reaction of cyclodextrin with reactants such as MO/β-CD and AV dye, is considered as the key step in photocatalytic degradation in MO suspension containing β-CD [57]. An electron is rapidly injected from the excited dye to the conduction band. The dye (AV) and dye cation ($AV^+$) radical then undergo decoloration (Eqs. (vii)–(ix)) [58,59]

$$MO + \beta\text{-CD} \longrightarrow MO/\beta\text{-CD} \quad \text{(i)}$$

$$AV + MO/\beta\text{-CD} \longrightarrow MO/\beta\text{-CD}^{\cdot}AV \quad \text{(ii)}$$

$$MO/\beta\text{-CD}^{\cdot}AV + h\nu \longrightarrow MO/\beta\text{-CD}^{\cdot 1}AV^{*} + MO/\beta\text{-CD}^{\cdot 3}AV^{*} \quad \text{(iii)}$$

$$MO/\beta\text{-CD}^{\cdot 3}AV^{*} \longrightarrow (e)\ MO/\beta\text{-CD} + AV^{\cdot +} \quad \text{(iv)}$$

$$MO/\beta\text{-CD}^{\cdot}AV^{*} + O_2 \longrightarrow MO/\beta\text{-CD}^{\cdot}AV + {}^1O_2 \quad \text{(v)}$$

$$(e)\ MO/\beta\text{-CD} + O_2 \longrightarrow MO/\beta\text{-CD} + O_2^{-} \quad \text{(vi)}$$

$$AV^{\cdot +} \longrightarrow \text{Products} \quad \text{(vii)}$$

$$AV + {}^1O_2 \longrightarrow \text{Products} \quad \text{(viii)}$$

$$AV + {}^{\cdot}O_2^{-} \longrightarrow \text{Products} \quad \text{(ix)}$$

Based on the above results, we conclude that the enhancement of photodecoloration of AV dye mainly results due to the enhanced adsorption of AV dye on MO surface and moderate inclusion depth of AV dye in the β-CD cavity. Since β-CD can include AV dye into its cavity and is adsorbed onto the surface of MO, it could play a role as "bridge" or "channel" for AV dye molecules to get onto the MO surface and accumulate in higher concentrations, which makes AV dye molecules decoloration more easily in the presence of hydroxyl radicals produced during photocatalytic decoloration processes [60,61].

## 4. Conclusion

The photodecoloration of AV dye on $TiO_2$/β-CD and ZnO/β-CD systems under UV light have been successfully studied and the results are compared with bare $TiO_2$ and ZnO. These studies indicate that $TiO_2$/β-CD and ZnO/β-CD systems possess good photodecoloration ability which may be due to the formation of inclusion complex between AV dye and β-CD. The catalysts were characterized by XRD, FE-SEM, and UV-DRS analyses. FT-IR, UV–visible, and $^1$H NMR studies confirm the formation of inclusion complex. $^1$H NMR results showed that the phenyl ring of AV dye is protruded into the β-CD cavity. Furthermore, among $TiO_2$/β-CD and ZnO/β-CD systems, ZnO/β-CD is having good photodecoloration ability than the $TiO_2$/β-CD. This is due to large absorption of light by ZnO than $TiO_2$ and also the band gap energy of ZnO/β-CD is higher than other catalysts and optical thickness of ZnO/β-CD is less than other systems.

## Acknowledgments

The authors thank the Management and the Principal of Ayya Nadar Janaki Ammal College, Sivakasi, India, for providing necessary facilities. Authors also thank the University Grants Commission, New Delhi, for providing financial support through UGC-Major Research Project [UGC – Ref. No. F. No. 38-22/2009 (SR) Dated: 19.12.2009]. Authors also acknowledged Bharadithasan University, Trichy, for recording FE-SEM and $^1$H NMR spectra and Department of Earth Science, Pondicherry University, Pondicherry, for recoding XRD spectrum.

## References

[1] M.C. Neves, J.M.F. Nogueira, T. Trindade, M.H. Mendonca, M.I. Pereira, O.C. Monteiro, Photosensitization of $TiO_2$ by $Ag_2S$ and its catalytic activity on phenol photodegradation, J. Photochem. Photobiol. A: Chem. 204 (2009) 168–173.
[2] A.P. Toor, A. Verma, C.K. Jotshi, J.P. Bajbai, V. Singh, Photocatalytic degradationof 3,4-dichlorophenol using $TiO_2$ in a shallow pond slurry reactor, Ind. J. Chem. Technol. 12 (2005) 75–81.
[3] G.M. Madhu, M.A. Lourdu Antony Raj, K. Vasantha Kumar Pai, S. Rao, Photodegradation of methylene blue using UV/$BaTiO_3$, UV/$H_2O_2$ and UV/$H_2O_2$/$BaTiO_3$ oxidation processes, Ind. J. Chem. Technol. 14 (2007) 139–144.
[4] A.C. Lee, R.H. Lin, C.Y. Yang, M.H. Lin, W.Y. Wang, Preparations and characterization of novel photocatalysts with mesoporous titanium dioxide ($TiO_2$) via a sol–gel method, Mater. Chem. Phys. 109 (2008) 275–280.
[5] M.T. Sulak, H.C. Yatmaz, Removal of textile dyes from aqueous solutions with eco-friendly biosorbent, Desalin. Water Treat. 37 (2012) 169–177.
[6] J.Z. Kong, A.D. Li, X.Y. Li, H.F. Zhai, W.Q. Zhang, Y.P. Gong, H. Li, D. Wu, Photo-degradation of methylene blue using Ta-doped ZnO nanoparticle, J. Solid State Chem. 183 (2010) 1359–1364.
[7] M.C. Yeber, J. Roderiguez, J. Freer, J. Baeza, N. Duran, H.D. Mansilla, Advanced oxidation of a pulp mill bleaching wastewater, Chemosphere 39 (1999) 1679–1688.
[8] M.A. Behnajady, N. Modirshahla, R. Hamzavi, Kinetic study on photocatalytic degradation of C.I. Acid Yellow 23 by ZnO photocatalyst, J. Hazard. Mater. B 133 (2006) 226–232.

[9] K. Woan, G. Pyrgiotakis, W. Sigmund, Photocatalytic carbon-nanotube-$TiO_2$ composites, Adv. Mater. 21 (2009) 2233–2239.
[10] T. Hirakawa, P.V. Kamat, Charge separation and catalytic activity of Ag@$TiO_2$ core–shell composite clusters under UV–irradiation, J. Am. Chem. Soc. 127 (2005) 3928–3934.
[11] D. Kannaiyan, E. Kim, N. Won, K.W. Kim, Y.H. Jang, M.A. Cha, D.Y. Ryu, S. Kim, D.H. Kim, On the synergistic coupling properties of composite CdS/$TiO_2$ nanoparticle arrays confined in nanopatterned hybrid thin films, J. Mater. Chem. 20 (2010) 677–682.
[12] S.H. Liu, L.X. Yang, S.H. Xu, S.L. Luo, Q.Y. Cai, Photocatalytic activities of C–N-doped $TiO_2$ nanotube array/carbon nanorod composite, Electrochem. Commun. 11 (2009) 1748–1751.
[13] S. Fukuzumi, T. Kojima, Photofunctional nanomaterials composed of multiporphyrins and carbon-based π-electron acceptors, J. Mater. Chem. 18 (2008) 1427–1439.
[14] Q.P. Luo, X. Yu, B.X. Lei, H.Y. Chen, D.B. Kuang, C.Y. Su, Reduced graphene oxide-hierarchical ZnO hollow sphere composites with enhanced photocurrent and photocatalytic activity, J. Phys. Chem. C 116 (2012) 8111–8117.
[15] X. Chen, S. Mao, Titanium dioxide nanomaterials: Synthesis, properties, modifications and applications, Chem. Rev. 107 (2007) 2891–2959.
[16] T. Tachikawa, S. Tojo, M. Fujitsuka, T. Majima, One-electron oxidation pathways during β-cyclodextrin-modified $TiO_2$ photocatalytic reactions, Chem. Eur. J. 12 (2006) 7585–7594.
[17] S. Anandan, M. Yoon, Photocatalytic degradation of Nile red using $TiO_2$–β cyclodextrin colloids, Catal. Commun. 5 (2004) 271–275.
[18] P. Lu, F. Wu, N. Deng, Enhancement of $TiO_2$ photocatalytic redox ability by β-cyclodextrin in suspended solutions, Appl. Catal. B: Environ. 53 (2004) 87–93.
[19] I. Willner, Y. Eichen, $TiO_2$ and CdS colloids stabilized by β-cyclodextrins: Tailored semiconductor–receptor systems as a means to control interfacial electron-transfer processes, J. Am. Chem. Soc. 109 (1987) 6862–6863.
[20] I. Willner, Y. Eichen, A.J. Frank, Tailored semiconductor–receptor colloids: Improved photosensitized $H_2$ evolution from water with $TiO_2$–β-cyclodextrin colloids, J. Am. Chem. Soc. 111 (1989) 1884–1886.
[21] I. Willner, Y. Eichen, B. Willner, Supramolecular semiconductor receptor assemblies: Improved electron transfer at $TiO_2$–β-cyclodextrin colloid interfaces, Res. Chem. Inter. 20 (1994) 681–700.
[22] N.M. Dimitrijevic, Z.V. Saponjic, D.M. Bartels, M.C. Thurnauer, D.M. Tiede, T. Rajhv, Revealing the nature of trapping sites in nanocrystalline titanium dioxide by selective surface modification, J. Phys. Chem. B 107 (2003) 7368–7375.
[23] T. Sano, E. Puzenat, C. Guillard, C. Geantet, S. Matsuzawa, Degradation of $C_2H_2$ with modified-$TiO_2$ photocatalysts under visible light irradiation, J. Mol. Catal. A 284 (2008) 127–133.
[24] Y.S. Ma, C.N. Chang, Y.P. Chiang, H.F. Sung, A.C. Chao, Photocatalytic degradation of lignin using Pt/$TiO_2$ as the catalyst, Chemosphere 71 (2008) 998–1004.
[25] D. Jiang, Y. Xu, D. Wu, Y. Sun, Visible-light responsive dye-modified $TiO_2$ photocatalyst, J. Solid State Chem. 181 (2008) 593–602.
[26] Y. Arai, K. Tanaka, A.L. Khlaifat, Photocatalysis of $SiO_2$-loaded $TiO_2$, J. Mol. Catal. A 243 (2006) 85–88.
[27] R. Qiu, D. Zhang, Y. Mo, L. Song, E. Brewer, X. Huang, Y. Xiong, Photocatalytic activity of polymer-modified ZnO under visible light irradiation, J. Hazard. Mater. B 156 (2008) 80–85.
[28] J.Z. Kong, A.D. Li, X.Y. Li, H.F. Zhai, W.Q. Zhang, Y.P. Gong, H. Li, D. Wu, Photo-degradation of methylene blue using Ta-doped ZnO nanoparticle, J. Solid State Chem. 183 (2011) 1359–1364.
[29] B. Li, Y. Wang, Synthesis, microstructure, and photocatalysis of ZnO/CdS nano-heterostructure, J. Phys. Chem. Solids 72 (2011) 1165–1169.
[30] N.M. Dimitrijevic, T. Rajh, Z.V. Saponjic, L. de la Garza, D.M. Tiede, Light-induced charge separation and redox chemistry at the surface of $TiO_2$/host-guest hybrid nanoparticles, J. Phys. Chem. B 108 (2004) 9105–9110.
[31] J. Feng, A. Miedaner, P. Ahrenkiel, M.E. Himmel, C. Curtis, D. Ginley, Self-assembly of photoactive $TiO_2$-cyclodextrin wires, J. Am. Chem. Soc. 12 (2005) 14968–14969.
[32] P. Velusamy, S. Rajalakshmi, S. Pitchaimuthu, N. Kannan, Photodecolouration of organic dyes on β-cyclodextrin modified ZnO as catalyst, Ind. J. Environ. Protect. 31 (2011) 801–809.
[33] P. Velusamy, S. Pitchaimuthu, S. Rajalakshmi, N. Kannan, Modification of the photocatalytic activity of $TiO_2$ by β-cyclodextrin in decoloration of ethyl violet dye, J. Adv. Res. accepted manuscript.
[34] K. Pitchumani, P. Velusamy, C. Srinivasan, Selectivity in sodium borohydride reduction of coumarin encapsulated in β-cyclodextrin, Tetrahedron 50 (1994) 12979–12988.
[35] P. Velusamy, Study of Thermal and Photochemical Reactions in Cyclodextrin, Ph.D. Thesis submitted to Madurai Kamaraj University, Madurai, May 1998, p. 50.
[36] E. Guivarch, S. Trevin, C. Lahitte, M.A. Oturan, Degradation of azo dyes in water by electro-Fenton process, Environ. Chem. Lett. 1 (2003) 38–44.
[37] R. Velmurugan, M. Swaminathan, An efficient nano structured ZnO for dye sensitized degradation of Reactive Red 120 dye under solarlight, Sol. Energy Mater. Sol. Cell 95 (2011) 942–950.
[38] G. Wang, F. Wu, X. Zhang, M. Luo, N. Deng, Enhanced photodegradation of bisphenol A in the presence of β-cyclodextrin under UV light, J. Chem. Technol. Biotechnol. 81 (2006) 805–811.
[39] K. Pitchumani, P. Velusamy, H. Shayira Banu, C. Srinivasan, A novel photorearrangement of benzyl sulfone encapsulated in β-cyclodextrin, Tetrahedron Lett. 36 (1995) 1149–1152.
[40] M. Chen, G. Diao, E. Zhang, Study of inclusion complex of β-cyclodextrin and nitrobenzene, Chemosphere 63 (2006) 522–529.
[41] G.L. Puma, P.L. Yue, A laminar falling Þlm slurry photocatalytic reactor. Part II experimental validation of the model, Chem. Eng. Sci. 53 (1998) 3007–3021.
[42] G.L. Puma, P.L. Yue, A novel fountain photocatalytic reactor: Model development and experimental validation, Chem. Eng. Sci. 56 (2001) 2733–2744.
[43] M.A. Salem, A.F. Al-Ghonemiy, A.B. Zaki, Photocatalytic degradation of Allura red and Quinoline yellow with Polyaniline/$TiO_2$ nanocomposite, Appl. Catal. B: Environ. 91 (2009) 59–66.
[44] S.K. Kansal, M. Singh, D. Sud, Studies on $TiO_2$/ZnO photocatalysed degradation of lignin, J. Hazard. Mater. 153 (2008) 412–417.
[45] I. Muthuvel, M. Swaminathan, Highly solar active Fe (III) immobilised alumina for the degradation of Acid Violet 7, Sol. Energy Mater. Sol. Cell 92 (2008) 857–863.
[46] S. Irmak, E. Kusvuran, O. Erbatur, Degradation of 4-chloro-2-methylphenol in aqueous solution by UV irradiation in the presence of titanium dioxide, Appl. Catal. B: Environ. 54 (2004) 85–91.
[47] S.X. Li, S.J. Cai, F.Y. Zheng, Self assembled $TiO_2$ with 5-sulfosalicylic acid for improvement its surface properties and photodegradation activity of dye, Dyes Pigments 95 (2012) 188–193.
[48] N. Sobana, M. Swaminathan, The effect of operational parameters on the photocatalytic degradation of acid red 18 by ZnO, Sep. Purif. Technol. 56 (2007) 101–107.
[49] C. Karunakaran, P. Anilkumar, Photooxidation of iodide ion on immobilized semiconductor powders, Sol. Energy Mater. Sol. Cell 92 (2008) 490–494.

[50] J. Fernandez, J. Kiwi, C. Lizama, J. Freer, J. Baeza, H.D. Mansilla, Factorial experimental design of Orange II photocatalytic discolouration, J. Photochem. Photobiol. A: Chem. 151 (2002) 213–219.
[51] O.E. Kartal, M. Erol, H. Oguz, Photocatalytic destruction of phenol by $TiO_2$ powders, Chem. Eng. Technol. 24 (2001) 6.
[52] Y. Chen, Z. Sun, Y. Yang, Q. Ke, Heterogeneous photocatalytic oxidation of polyvinyl alcohol in water, J. Photochem. Photobiol. A: Chem. 142 (2001) 85–89.
[53] M.R. Sohrabi, M. Ghavami, Comparison of Direct Yellow 12 dye degradation efficiency using UV/semiconductor and UV/$H_2O_2$/semiconductor systems, Desalination 252 (2010) 157–162.
[54] M. Muruganandham, M. Swaminathan, Photocatalytic decolourisation and degradation of Reactive Orange 4 by $TiO_2$–UV process, Dyes Pigments 68 (2006) 133–142.
[55] S. Sakthivel, B. Neppolian, M.V. Shankar, B. Arabindoo, M. Palanichamy, V. Murugesan, Solar photocatalytic degradation of azo dye: Comparison of photocatalytic efficiency of ZnO and $TiO_2$, Sol. Energy Mater. Sol. Cell 77 (2003) 65–82.
[56] W. Dong, C.W. Lee, X. Lu, Y. Sun, W. Hua, G. Zhuang, S. Zhang, J. Chen, H. Hou, D. Zhao, Synchronous role of coupled adsorption and photocatalytic oxidation on ordered mesoporous anatase $TiO_2$–$SiO_2$ nanocomposites generating excellent degradation activity of RhB dye, Appl. Catal. B: Environ. 95 (2010) 197–207.
[57] X. Zhang, F. Wu, N. Deng, Efficient photodegradation of dyes using light-induced self assembly $TiO_2$/β-cyclodextrin hybrid nanoparticles under visible light irradiation, J. Hazard. Mater. B 185 (2011) 117–123.
[58] M.R. Hoffmann, S.T. Martin, W. Choi, D.W. Bahnemann, Environmental applications of semiconductor photocatalysis, Chem. Rev. 95 (1995) 69–96.
[59] D.P. Macwan, P.N. Dave, S. Chaturvedi, A review on nano-$TiO_2$ sol–gel type syntheses and its applications, J. Mater. Sci. 46 (2011) 3669–3686.
[60] G. Wang, F. Wu, X. Zhang, M. Luo, N. Deng, Enhanced $TiO_2$ photocatalytic degradation of bisphenol E by β-cyclodextrin in suspended solutions, J. Hazard. Mater. B 133 (2006) 85–91.
[61] G. Wang, F. Wu, X. Zhang, M. Luo, N. Deng, Enhanced $TiO_2$ photocatalytic degradation of bisphenol A by β-cyclodextrin in suspended solutions, J. Photochem. Photobiol. A: Chem. 179 (2006) 49–56.